CrystEngComm

Accepted Manuscript

ROYAL SOCIETY OF CHEMISTRY

www.rsc.org/crystengcomm

Cite this: DOI: 10.1039/coxx00000x

www.rsc.org/chemcom COMMUNICATIONS

Tuning pore size in a zirconium-tricarboxylate metal-organic framework

Weibin Liang,[a] Hubert Chevreau,[b] Florence Ragon,[a] Peter D. Southon,[a] Vanessa K. Peterson,[b] and Deanna M. D'Alessandro*[a]

Received (in XXX, XXX) Xth XXXXXXXXX 20XX, Accepted Xth XXXXXXXXX 20XX
DOI: 10.1039/b000000x

The water-stable zirconium-tricarboxylate series of frameworks, $[Zr_6O_4(OH)_4(X)_6(btc)_2].nH_2O$, where X = formate (F), acetate (A), or propionate (P), exhibit tunable porosity by virtue of systematic modulation of the chain length of the monocarboxylate ligand X. This modification not only impacts the pore size of the framework, but provides an important avenue for the construction of mixed-linker MOFs.

Metal-organic frameworks (MOFs) are a class of porous materials composed of organic struts and inorganic nodes,[1] which have been tailored to applications including gas storage,[2] guest separation,[3] catalysis,[4] sensors,[5] and drug delivery.[6, 7] One of the most attractive aspects of MOFs is the tunability of their properties, achieved through synthetic modification of their secondary building units (SBU) and bridging linkers, allowing the introduction of tailored functionality to the structure.[8, 9] While the low stability of many MOFs presents a limitation to their use in industrial processes,[10] zirconium-based frameworks have considerable potential for such applications owing to their exceptional chemical, hydrothermal, and mechanical stabilities.[11] These advantageous properties are attributed to the significant covalent character of the Zr^{IV}-O bonds which are often present in carboxylate-bridged Zr SBUs,[11] with such building units regarded as some of the most stable for MOF construction.

Since the first report of a Zr-based MOF, $[Zr_6O_4(OH)_4(bdc)_6]$ (where bdc = 1,4-benzenedicarboxylate, also known as UiO-66),[12] only a handful of new structures containing zirconium oxo clusters have been published, and these have contained predominantly di- and tetradentate ligands.[12-17]

The highly stable $Zr_6O_4(OH)_4(CO_2)_{12}$ SBU in $[Zr_6O_4(OH)_4(bdc)_6]$ is built from 6 Zr atoms each connected to two bdc linker units, resulting in 8-coordinate Zr^{IV}. Each SBU is bound by 12 carboxylate groups from 12 different bdc ligands to create a three dimensional uninodal framework with fcu architecture.[12] The stability of the $Zr_6O_4(OH)_4(CO_2)_{12}$ SBU has enabled significant modification of this framework. Isostructural materials have been created using extended ligands, including $[Zr_6O_4(OH)_4(bpdc)_6]$ and $[Zr_6O_4(OH)_4(tpdc)_6]$ containing 4,4'-biphenyldicarboxylate (bpdc) and 4,4',4''-triphenyldicarboxylate (tpdc),[12] although these show significantly lower stabilities than $[Zr_6O_4(OH)_4(bdc)_6]$. Further modifications via post-synthetic methodologies have introduced functional groups onto the ligands with the aim of targeting specific applications, and have produced a range of extensively-studied $[Zr_6O_4(OH)_4(bdc)_6]$ derivatives.[11]

The stability of the zirconium oxo cluster supports a reduction in the connectivity of the Zr_6 core from the original 12 in $[Zr_6O_4(OH)_4(bdc)_6]$. Porphyrin-based ligands have been used to create MOFs with 8-connected Zr_6 clusters, such as the (4,8)-connected PCN-222 (a csq-a topology)[15] as well as the (4,12)-connected PCN-521 and PCN-523 materials (with a flu topology),[18] and also the (4,6)-connected PCN-224 (a she net) with a 6-connected Zr_6 core.[16] Further, the PCN-221 material (with a ftw topology)[14] also features a porphyrin-based ligand and contains a 12-connected cubic Zr_8 core in place of the well-known octahedral Zr_6 core.

The $[Zr_6O_4(OH)_4(bdc)_6]$ structure is comprised of a central octahedral cage with 8 face-sharing supertetrahedra (ST).[12] The four vertices of the ST are each occupied by a Zr_6-oxo cluster with edges formed by the bdc ligands. Instead of edge-occupying bdc, such ST can also be built from face-located btc (1,3,5-benzenetricarboxylate) ligands, such as in the MIL-100(Fe) and MIL-101(Fe) materials.[18, 19] Inspired by this idea, we focused on constructing porous zirconium MOFs constructed from face-capping ST using zirconium oxo clusters and the tridentate btc ligand.

We report herein the solvothermal synthesis of a series of three isostructural zirconium-btc MOFs, each containing Zr_6 core with general formula $[Zr_6O_4(OH)_4(X)_6(btc)_2]$, where X = formate (F), acetate (A), or propionate (P). Importantly, we demonstrate that the monocarboxylic ligand controls pore size and allows modulation of gas uptake properties, important for a wide range of applications, most notably gas storage.

We obtained $[Zr_6O_4(OH)_4(A)_6(btc)_2].nH_2O$ (denoted here as **A**.nH_2O) as a crystalline powder after attempts at obtaining single crystals by varying synthesis parameters (temperature, time, stoichiometry, and concentration, see ESI) were unsuccessful. **A**.nH_2O, with formula $[Zr_6O_4(OH)_4(O_2C_2H_3)_6(btc)_2].32H_2O$ (n estimated by thermogravimetric analysis, see ESI), was stable to activation (desolvation) and the structure of **A** was solved *ab-initio* using high intensity synchrotron powder X-ray diffraction data (see ESI). **A** crystallises in the cubic space group $Fd\bar{3}m$ with unit cell parameters a = 35.2675(11) Å and cell volume V = 43865.6(40) Å^3 (Fig. 1). The framework consists of

$Zr_6O_4(OH)_4(CO)_{12}$ clusters linked by tridentate btc ligands, forming ST, while the btc ligands occupy the faces of the ST. Regarding the $Zr_6O_4(OH)_4(CO)_{12}$ clusters, only six of the carboxylate functionalities (of the twelve in the core) are bridged by the carboxylates from the btc ligands, with the remaining six occupied by the acetate groups (Fig. 1a), as distinct from the 12-, 8- and 6-connections to framework linker units of Zr_6 clusters in other zirconium oxo cluster-containing MOFs.[12,14,15] The structure of **A** can be considered in terms of ST, with diameter ≈ 6 Å, that extend into a three-dimensional *β*-cristobalite zeolite network through connection of the ST vertices (Fig. 1d).[20, 21] This arrangement leads to the formation of large, approximately spherical cavities with diameter ≈ 16 Å (Fig. 1f), capped by four ST faces. The large pores are accessible through four hexagonal windows with apertures of approximately 10 Å (Fig. 1e). Compared to the ST in $[Zr_6O_4(OH)_4(bdc)_6]$, the approximate diameter of the ST in **A** are 20% smaller (6 Å *cf.* 7.5 Å). Very recently the MOF $[Zr_6O_4(OH)_4(O_2CH)_6(btc)_2]$, denoted MOF-808, was reported by Furukawa *et al.*[22] using single crystal X-ray analysis. MOF-808 is isostructural to **A** and is the material $[Zr_6O_4(OH)_4(F)_6(btc)_2]$ reported in the present work.

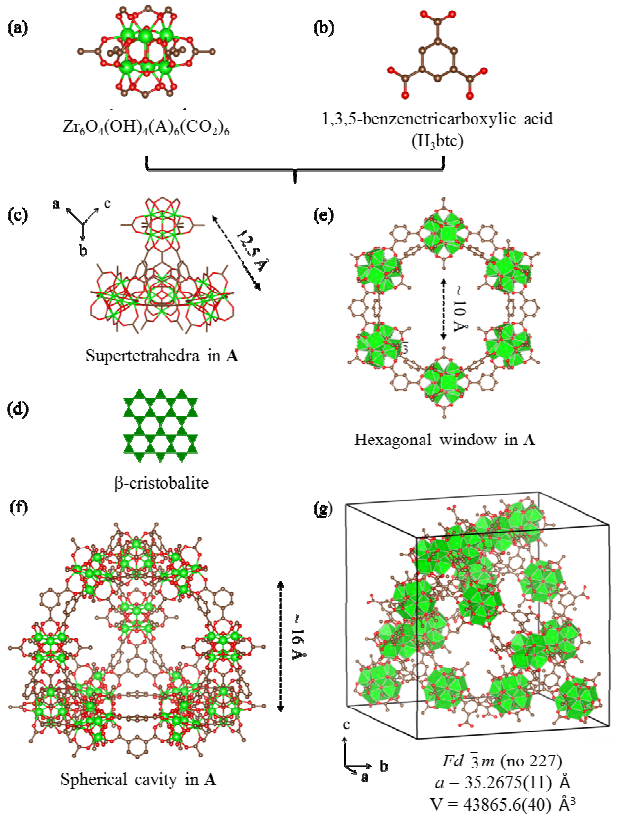

Fig. 1 (a) The $Zr_6O_4(OH)_4(AcO)_6(CO_2)_6$ cluster in **A**. (b) H_3btc (c) supertetrahedra of **A** (d) schematic of the β-cristobalite topology (e) hexagonal window in **A** (f) approximately spherical cavity in **A**; (g) unit cell of **A**. Color scheme: Zr shown in green, O in red, C in grey. H are omitted for clarity.

Variable temperature X-ray powder diffraction (XRPD) analysis shows that **A** exhibits relatively lower thermal stability (stable to approximately 270 °C, see ESI) than other Zr-based MOFs (450 °C for the UiO series and 550 °C for the MIL-140 series).[12, 16] Despite the lower thermal stability of **A,** the MOF exhibits extraordinary chemical stability relative to $[Zr_6O_4(OH)_4(bdc)_6]$. Powder X-ray diffraction shows that the structure of **A** is retained upon immersion in boiling H_2O, concentrated HCl (32%), and in aqueous solution of pH 10 for 24 h (Fig. 2), suggesting that no phase transition or framework collapse occurs during these treatments (ESI).

Monodentate modulators, typically with similar chemical functionalities to the polydentate linker molecules, are used in MOF preparation primarily to regulate crystal growth.[23] For Zr-based MOFs, modulators such as acetic acid were first introduced by Schaatte *et al.* to improve the crystallinity of the UiO-type isoreticular frameworks.[24] However, one study reported that a modulator (functionalised isophthalic acid) can also be used to partially replace the ligands (terphenyl-3,3″,5,5″-tetracarboxylate) in a MOF (PCN-125), creating mesopores inside the crystals.[25] More recent reports have demonstrated that monocarboxylic acids can partially substitute the dicarboxylate linkers from pristine UiO-66 and UiO-67, generating defect structures with higher porosities.[26-28] As a key structural feature in **A**, the presence of coordinated acetate has been confirmed experimentally (*vide infra*), and is integral to the structure, serving to stabilise the SBU. Prior to further analysis, **A** was washed with DMF, acetone, and methanol, and then dried under vacuum. Fourier transform infrared (FTIR) measurements confirmed the full removal of free acid acetate (1710 cm^{-1}) with the band at 1660 cm^{-1} indicating coordinated acetate (see ESI).

^{1}H NMR studies of the alkaline-digested sample indicated the absence of DMF molecules and the presence of acetic acid in a 2.7:1: ratio with the btc linker, with the ~ 1650 cm^{-1} peak in the FTIR spectrum of the activated sample attributed to the coordinated acetate anions (see the ESI). Taken together with the elemental analysis, the proposed structure of **A** determined from Rietveld refinement using synchrotron powder X-ray diffraction (PXRD) data, $[Zr_6O_4(OH)_4(O_2CCH_3)_6(btc)_2].32H_2O$, is supported qualitatively and quantitatively.

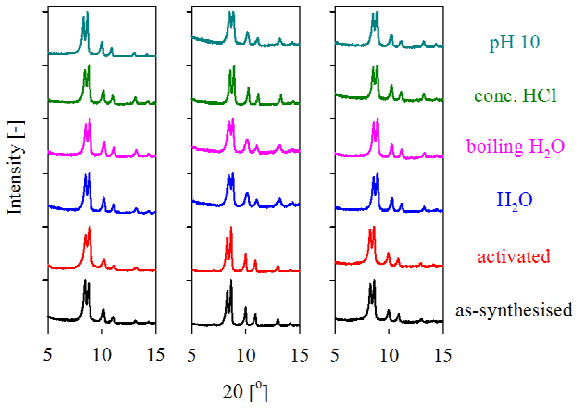

Fig. 2 XRPD patterns showing the stability of **A** (left), **F** (middle), and **P** (right), upon treatment in H_2O, boiling H_2O, concentrated HCl (32%) and pH 10 aqueous solution for 24 h.

A critical aspect of the **A** structure is the orientation of the acetate groups pointing toward the centre of the cavities. This characteristic was exploited here to modify the pore size by varying the monocarboxylate ligand. Using proprionic and formic acid in place of acetic acid in our synthesis yielded the isostructural series $[Zr_6O_4(OH)_4(X)_6(btc)_2]$, where X = formate

(F), acetate (A), or propionate (P). These compounds are termed **F**, **A**, and **P**, respectively. The compounds **F** and **P** are robust to activation in a similar manner to **A**, and the isostructural nature of the activated series is confirmed through Le Bail analysis of PXRD data (ESI).

The lattice parameters are a = 35.3732(16) Å for **F**, 35.3854(17) Å for **P** and 35.3049(15) for **A,** the slight differences are likely to result from variations in the degree of residual pore solvent molecules being present. Variable temperature PXRD and chemical stability tests confirmed that both **F** and **P** have similar hydrothermal and chemical stabilities to **A** (Fig. 2 and ESI).

The variation of the monocarboxylate ligand chain length in **F**, **A**, and **P** had a marked influence on the porosity of the solid. The tunability of the porosity has important implications for future applications of the framework, and we demonstrate a systematic strategy here for controlled tuning of the pore size. To assess the optimal activation temperature for porosity determination, ~100 mg samples of **A** (from the same batch) were activated overnight at different temperatures (100, 140, 180 and 220 °C) under dynamic vacuum (~ 10^{-6} bar). N_2 adsorption analyses at 77 K indicated that high-temperature activation (> 140 °C) resulted in a decline in surface area, which was attributed to framework collapse (see ESI). A temperature of 100 °C was subsequently selected to activate **A**. Compared to the 100 °C-activated **A**, ^{1}H NMR analysis revealed a lower amount of acetate in the 180 and 220 °C-activated **A,** with the ratio of acetate to btc decreasing by ~ 50% (see ESI). In addition, FTIR measurements for 180 and 220 °C-activated **A** indicated the absence of coordinated acetate (1660 cm^{-1}) and the presence of the stretching band related to the free acid (1710 cm^{-1}) (see ESI). These results suggest that the mechanism for framework collapse involves removal of coordinated acetate groups from **A**, indicating that it is these groups that underpin the extraordinary chemical stability of the material.

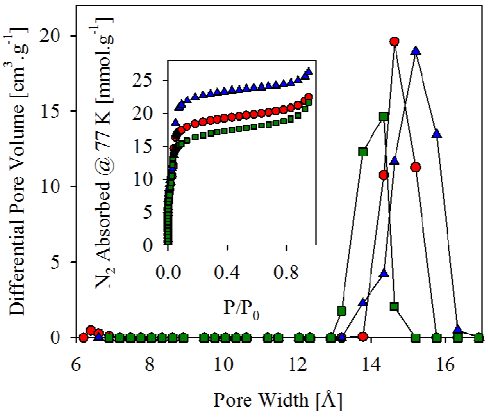

Fig. 3 Pore size distributions and N_2 adsorption isotherms (inset) for **A** (red), **F** (blue), and **P** (green).

N_2 adsorption isotherms at 77 K for **F, A,** and **P** are typical type I, with a step at P/P_0 ~ 0.03 (Fig. 3). The resulting Brunauer-Emmett-Teller (BET) and Langmuir surface areas, along with the total pore volume (in parentheses) were found to be 1606(10) and 1864.4(5) $m^2.g^{-1}$(0.78 $cm^3.g^{-1}$) for **A**, 2330(64) and 2770.4(74) $m^2.g^{-1}$(0.90 $cm^3.g^{-1}$) for **F**, and 1408(7) and 1633.2(2) $m^2.g^{-1}$ (0.75 $cm^3.g^{-1}$) for **P**, indicating an increase in surface area and pore volume with a decrease in chain length.

Non-local density functional theory (NLDFT, based on the *Carbon slit-pore model* in the ASAP2020 software package, Micromeritics Instruments Inc.) calculations indicated that the average diameter of the pores varies as a function of the chain length, being ~ 15.2 Å in **F,** ~ 14.2 Å in P, and ~14.6 Å in **A** (Fig. 3). Attempts at producing crystalline products using benzoic and isobutyric acids were unsuccessful (ESI), presumably owing to the relatively bulky size of monocarboxylates and the relatively small pore diameter of the structure.

In summary, the series of porous zirconium-tricarboxylate metal-organic frameworks $[Zr_6O_4(OH)_4(X)_6(btc)_2]$ were synthesised, and exhibited pronounced chemical stability. Importantly, we demonstrate tunable porosity through modulation of the monocarboxlic acid chain length, where the monocarboxylic acid serves as a monodentate ligand for Zr_6 cluster construction. This work opens up an important avenue for the future construction of mixed-linker MOFs. For example, the benzoate ligands in the MOF NU-1000 can be replaced by –OH groups via a solvent-assisted ligand incorporation strategy.[29, 30] Experiments are currently underway to explore the possibility of pore space functionalisation within $[Zr_6O_4(OH)_4(X)_6(btc)_2]$ using similar strategies.

This work was funded by Science and Industry Endowment Fund (SIEF). Use of the Advanced Photon Source was supported by the U.S. Department of Energy, Office of Science, Office of Basic Energy Sciences, under Contract No. DE-AC02-06CH11357; we thank Dr. Gregory J. Halder for beamline support. Travel to the APS was funded by the International Synchrotron Access Program (ISAP) managed by the Australian Synchrotron and funded by the Australian Government.

Notes and references

[a] *School of Chemistry, Building F1, University of Sydney, NSW, 2006, Australia; Tel: 61 (2)93513777; E-mail: deanna.dalessandro@sydney.edu.au*

b Australian Nuclear Science and Technology Organisation, Kirrawee DC, NSW 2232, Australia.

† Electronic Supplementary Information (ESI) available: The Supporting Information contains the synthetic procedure for the $Zr_6O_4(OH)_4(A)_6(btc)_2$ material, together with details on the crystal-structure determination method. Elemental analysis, thermogravimetric analysis, variable temperature powder X-ray diffraction analysis, infrared spectroscopy spectra, ^{1}H nuclear magnetic resonance spectra, and N_2 sorption measurements are also provided. See DOI: 10.1039/b000000x/

1. M. O'Keeffe and O. M. Yaghi, *Chem. Rev.*, 2012, **112**, 675-702.
2. D. M. D'Alessandro, B. Smit and J. R. Long, *Angew. Chem. Int. Ed. Engl.*, 2010, **49**, 6058-6082.
3. Z. R. Herm, E. D. Bloch and J. R. Long, *Chem. Mater.*, 2013, **26**, 323-338.
4. M. Yoon, R. Srirambalaji and K. Kim, *Chem. Rev.*, 2012, **112**, 1196-1231.
5. C. Wang, D. Liu and W. Lin, *J. Am. Chem. Soc.*, 2013, **135**, 13222-13234.
6. P. Horcajada, T. Chalati, C. Serre, B. Gillet, C. Sebrie, T. Baati, J. F. Eubank, D. Heurtaux, P. Clayette, C. Kreuz, J.-S. Chang, Y. K. Hwang, V. Marsaud, P.-N. Bories, L. Cynober, S. Gil, G. Ferey, P. Couvreur and R. Gref, *Nat. Mater.*, 2010, **9**, 172-178.
7. J. Della Rocca, D. Liu and W. Lin, *Acc. Chem. Res.*, 2011, **44**, 957-968.
8. F. A. Almeida Paz, J. Klinowski, S. M. F. Vilela, J. P. C. Tomé, J. A. S. Cavaleiro and J. Rocha, *Chem. Soc. Rev.*, 2012, **41**,

1088-1110.
9. J. J. Perry Vi, J. A. Perman and M. J. Zaworotko, *Chem. Soc. Rev.*, 2009, **38**, 1400-1417.
10. K. A. Cychosz and A. J. Matzger, *Langmuir*, 2010, **26**, 17198-17202.
11. M. Kim and S. M. Cohen, *CrystEngComm*, 2012, **14**, 4096-4104.
12. J. H. Cavka, S. Jakobsen, U. Olsbye, N. Guillou, C. Lamberti, S. Bordiga and K. P. Lillerud, *J. Am. Chem. Soc.*, 2008, **130**, 13850-13851.
13. D. Feng, H.-L. Jiang, Y.-P. Chen, Z.-Y. Gu, Z. Wei and H.-C. Zhou, *Inorg. Chem.*, 2013, **52**, 12661-12667.
14. D. Feng, Z. Y. Gu, J. R. Li, H. L. Jiang, Z. Wei and H. C. Zhou, *Angew. Chem. Int. Ed.*, 2012, **51**, 10307-10310.
15. D. Feng, W.-C. Chung, Z. Wei, Z.-Y. Gu, H.-L. Jiang, Y.-P. Chen, D. J. Darensbourg and H.-C. Zhou, *J. Am. Chem. Soc.*, 2013, **135**, 17105-17110.
16. V. Guillerm, F. Ragon, M. Dan-Hardi, T. Devic, M. Vishnuvarthan, B. Campo, A. Vimont, G. Clet, Q. Yang, G. Maurin, G. Ferey, A. Vittadini, S. Gross and C. Serre, *Angew. Chem. Int. Ed.*, 2012, **51**, 9267-9271.
17. M. Zhang, Y.-P. Chen, M. Bosch, T. Gentle, III, K. Wang, D. Feng, Z. U. Wang and H.-C. Zhou, *Angew. Chem. Int. Ed.*, 2014, **53**, 815-818.
18. G. Ferey, C. Mellot-Draznieks, C. Serre, F. Millange, J. Dutour, S. Surble and I. Margiolaki, *Science*, 2005, **309**, 2040-2042.
19. G. Ferey, C. Serre, C. Mellot-Draznieks, F. Millange, S. Surble, J. Dutour and I. Margiolaki, *Angew. Chem. Int. Ed.*, 2004, **43**, 6296-6301.
20. H. Chevreau, T. Devic, F. Salles, G. Maurin, N. Stock and C. Serre, *Angew. Chem. Int. Ed.*, 2013, **52**, 5056-5060.
21. M. Frigoli, R. El Osta, J. Marrot, M. E. Medina, R. I. Walton and F. Millange, *Eur. J. Inorg. Chem.*, 2013, **2013**, 1138-1141.
22. H. Furukawa, F. Gándara, Y.-B. Zhang, J. Jiang, W. L. Queen, M. R. Hudson and O. M. Yaghi, *J. Am. Chem. Soc.*, 2014, **136**, 4369-4381.
23. M. Sindoro, N. Yanai, A.-Y. Jee and S. Granick, *Acc. Chem. Res.*, 2014, **47**, 459-469.
24. A. Schaate, P. Roy, A. Godt, J. Lippke, F. Waltz, M. Wiebcke and P. Behrens, *Chem. -Eur. J.*, 2011, **17**, 6643-6651.
25. J. Park, Z. U. Wang, L.-B. Sun, Y.-P. Chen and H.-C. Zhou, *J. Am. Chem. Soc.*, 2012, **134**, 20110-20116.
26. F. Vermoortele, B. Bueken, G. Le Bars, B. Van de Voorde, M. Vandichel, K. Houthoofd, A. Vimont, M. Daturi, M. Waroquier, V. Van Speybroeck, C. Kirschhock and D. E. De Vos, *J. Am. Chem. Soc.*, 2013, **135**, 11465-11468.
27. H. Wu, Y. S. Chua, V. Krungleviciute, M. Tyagi, P. Chen, T. Yildirim and W. Zhou, *J. Am. Chem. Soc.*, 2013, **135**, 10525-10532.
28. P. Xydias, I. Spanopoulos, E. Klontzas, G. E. Froudakis and P. N. Trikalitis, *Inorg. Chem.*, 2013, **53**, 679-681.
29. P. Deria, J. E. Mondloch, E. Tylianakis, P. Ghosh, W. Bury, R. Q. Snurr, J. T. Hupp and O. K. Farha, *J. Am. Chem. Soc.*, 2013, **135**, 16801-16804.
30. P. Deria, W. Bury, J. T. Hupp and O. K. Farha, *Chem. Commun.*, 2014, **50**, 1965-1968.